International Conference on Plasma Physics

Joint Conference of
Fourth Kiev International Conference on Plasma Theory
and
Fourth International Congress on Waves and Instabilities in Plasmas

April 7 – 11, 1980
Nagoya, Japan

Fusion Research Association of Japan
Supported by
IUPAP and URSI

Stimulated Brillouin Scattering

Francis F. Chen
Electrical Sciences and Engineering Department
University of California
Los Angeles, California 90024

Abstract: The current status of theoretical and experimental understanding of stimulated Brillouin scattering in laser-plasma interactions is summarized.

1. Theory

Of all parametric instabilities predicted by theory, stimulated Brillouin scattering (SBS) has attracted the most experimental attention because of its possible threat to efficient light absorption. The interaction is described by the coupled equations (we use standard notation and follow the approach of Kruer[1]):

$$(\omega_o^2 + 2i\gamma_o\omega_o - \omega_p^2 - k_o^2c^2)\, E_o = \omega_p^2(\omega_o/\omega_2)(n_1/n_o)E_2 \qquad (1)$$

$$(\omega_2^2 + 2i\gamma_2\omega_2 - \omega_p^2 - k_2^2c^2)\, E_2 = \omega_p^2(\omega_2/\omega_o)(n_1/n_o)E_o \qquad (2)$$

$$(\omega_1^2 + 2i\gamma_i\omega_1 - k_1^2c_s^2)\, n_1 = (\omega_p^2/\omega_o\omega_2)(k_1^2/M)(E_oE_2/4\pi), \qquad (3)$$

where E_o, E_2, and n_1 or n_i are the amplitudes of the incident, reflected, and ion waves, respectively. The e.m. wave damping γ_o, γ_2 is usually negligible; but at the small T_e/T_i ratios usually encountered the ion Landau damping term in γ_i is the dominant one in (3). Thus, Eq. (3) gives

$$\frac{|n_1|}{n_o} \equiv \frac{\tilde{n}}{n} = \frac{e^2}{2mM}\,\frac{k_i^2}{\gamma_i\omega_i}\,\frac{E_oE_2}{\omega_o\omega_2}, \qquad (4)$$

which expresses the balance between ion damping and wave growth due to the ponderomotive force of E_o beating with E_2. Note that $\tilde{n}$ follows the spatial variation of the pump E_oE_2; the ion wave does not grow in the direction of $\underline{k}_i$ because it is highly damped. The slow spatial part of Eqs. (1) and (2) in steady state can be separated out to give

$$\partial E_2/\partial x = -C(\tilde{n}/n)E_o \qquad (5)$$

$$\partial E_o/\partial x = -C(\tilde{n}/n)E_2 \tag{6}$$

where
$$C = (\pi/2)(n/n_c)/\lambda_o' \ , \tag{7}$$

λ_o' being the local wavelength $\lambda_o\sqrt{\varepsilon}$. The interaction length is limited by focal depth, plasma thickness, or temperature or velocity gradients, which dephase the waves and cause turning points. Let the plasma be finite (x = 0 to L) and uniform. There are two interesting limits to this spatial problem. If $\tilde{n}/n$ is clamped at some saturation level by a nonlinear process, Eqs.(5) and (6) can be integrated from 0 to L with $\tilde{n}/n$ constant. Neglecting the noise level $E_2(L)$, one obtains the reflection coefficient R:

$$\left|\frac{E_2(0)}{E_o(0)}\right|^2 \equiv R = \tanh^2\alpha, \qquad \alpha = \underset{n}{\overset{\tilde{n}}{C\text{—}L}} = \frac{\pi}{2}\frac{n}{n_c}\frac{\tilde{n}}{n}\frac{L}{\lambda_o'} . \tag{8}$$

This is independent of I_o and represents saturated backscatter. For given n/n_c and $\tilde{n}/n$, however, R depends on L/λ_o; this is one reason long λ_o leads to low backscatter. When pump depletion is negligible (small α), expansion of (8) gives

$$R = \tanh^2\alpha \simeq \alpha^2 = \left(\frac{\pi}{2}\frac{n}{n_c}\frac{\tilde{n}}{n}\frac{L}{\lambda_o}\right)^2 , \tag{9}$$

which is identical with the Bragg scattering formula for a uniform grating: $R = (\tfrac{1}{2}\tilde{n}L\lambda_o r_o)^2$, $r_o \equiv e^2/mc^2$.

The other interesting case is when $\tilde{n}/n$ varies in space according to Eq. (4). There are now three coupled equations (4-6), which can also be integrated from x = 0 to L, giving

$$R(1 - R) = R_o(e^{g(1-R)} - R) , \tag{10}$$

where
$$g = \frac{1}{4}\frac{v_o^2}{v_e^2}\frac{n}{n_c}\frac{k_o L}{\sqrt{\varepsilon}}\frac{\omega_i}{\gamma_i}\left(1 + \frac{3T_i}{ZT_e}\right)^{-1} . \tag{11}$$

Here v_o is the peak quiver velocity, and R_o the noise level $I_2(L)/I_o(0)$, with $v_e^2 = KT_e/m$. Note that all three amplitudes decrease from x=0 to x=L. In the absence of pump depletion (small R), Eq. (10) becomes

$$R = R_o e^g , \tag{12}$$

showing exponential growth. This is identical to the linear-

theory formula[2]

$$P_s = P_n e^{2\gamma_o^2 L/c\gamma_i} , \quad \gamma_o = (v_o/c)(\omega_o/\omega_i)^{\frac{1}{2}}\Omega_{pi} , \tag{13}$$

P_n being the noise power and γ_o the "homogeneous" growth rate. When $3T_i/ZT_e$ is not small, SBS merges into Compton scattering, and Eq. (13) should be replaced by the kinetic-theory result[3]

$$P_s = P_n e^{2LIm(k)}, \quad Im(k) = k_o(v_o^2/c^2)Im\{\chi_e(1+\chi_i)/(1+\chi_e+\chi_i)\}. \tag{14}$$

For given (n/n_c) and (ω_i/γ_i), the growth factor g is seen to be proportional to $v_o^2 k_o \propto \lambda_o$, suggesting that long wavelength is worse. However, R is limited by more than just pump depletion, as Eq. (10) suggests, because γ_i is itself a function of R and I_o because of ion heating.

The energy given to ion waves in a region of length L is $LI_2(\omega_i/\omega_2) \simeq LRI_o(\omega_i/\omega_o)$ ergs/cm^{2}sec, as a consequence of quantum conservation (Manley-Rowe relation). How this affects γ_i depends on the model. If the energy is all given to the bulk of the ion distribution and convects away at the sound velocity c_s, we should equate $LRI_o(\omega_i/\omega_o)$ to $n_i KT_i c_s L$, obtaining

$$KT_i = \frac{RI_o\omega_i}{n_i c_s \omega_o} = \frac{2Z}{cn_c}\left(\frac{n_c}{n}\right)RI_o. \tag{15}$$

Here we have taken $\omega_i = 2k_o c_s$ and $n_i = n/Z$. As I_o and R increase, $ZT_e/3T_i$ decreases, raising the Landau damping rate γ_i exponentially. If this rate is used in Eqs. (10) and (11), R is found to saturate as L/λ_o is increased, and even more strongly as I_o is increased[1]. This effect is stronger with large λ_o (small n_c) simply because there are fewer ions to heat. The maximum T_i is obviously $\simeq T_e$. For this value, Eq. (15) gives[4]

$$R \to (v_e^2/v_o^2)(n/Zn_c) , \tag{16}$$

showing that $R(I_o)$ can eventually decrease.

More likely, the wave energy is given to a population n_h of trapped ions accelerated to a velocity $\simeq c_s$ with an effective temperature T_h. The energy loss is then $n_h KT_h c_s L$, and the same calculation can be made with the hot ions doing the Landau damping. For $n/n_c = 1/3$ and $L/\lambda_o = 50$, Kruer[1] finds that $R(I_o)$ saturates

at 37%. A more definite prescription for the transfer of wave energy to ions is given by the theory of nonlinear Landau damping Using this to compute γ_i self-consistently, Thomson and Mima[5] find that $R(I_o)$ maximizes at ≈50% and then decreases again. Computer simulations[1] show that saturation is ins nsitive to the detailed model, partly because of the self-correcting feature of ion heating, and partly because the heated ions tend to fall into a thermal distribution--a sort of high-frequency extension of the Langmuir paradox. Other saturation mechanisms will be discussed later, but ion heating seems to explain high intensity experiments adequately.

2. Experimental data

Solid target experiments have many parameters which affect the various ratios in g [Eq.(11)], notably L/λ_o: 1) spot size and focal position, 2) pulse length and shape, 3) f-number, 4) target shape and size, 5) M and $\bar{Z}$, 6) angle of incidence, 7) λ_o, and 8)I_o. Furthermore, the Doppler blueshift due to plasma expension, and sidescatter and specular reflection complicate data interpretation. Recent measurements of back reflection through the focussing optics are shown indiscriminately vs. I_o in Fig. 1. Included are data from Livermore[6], Los Alamos[7], Osaka[5,8], Rutherford[9], Garching[10], Palaiseau[11], and Quebec INRS[12]. In many of these experiments, time-integrated spectra were obtained, showing broad, redshifted peaks. In flat-target experiments it is possible to subtract the blue contribution of plasma drift by varying the angle of incidence. In some cases the redshifted sidescatter contribution was also recorded. Large focal spots and long pulses, which tend to produce large L/λ_o, give larger R. Though many different experimental conditions are grouped together in Fig. 1, it is possible to draw two conclusions: backscatter can be significant, and 10.6-μm results (in red) tend to give lower SBS than 1.06-1.3 μm results (in blue and green). This is in apparent agreement with the predictions that small L/λ_o and small ion heat capacity lead to small R; however, recent results at 0.53 μm from several labs seem to contradict this trend, possibly because of strong classical absorption.

In Fig. 2 we show results from experiments specifically design-

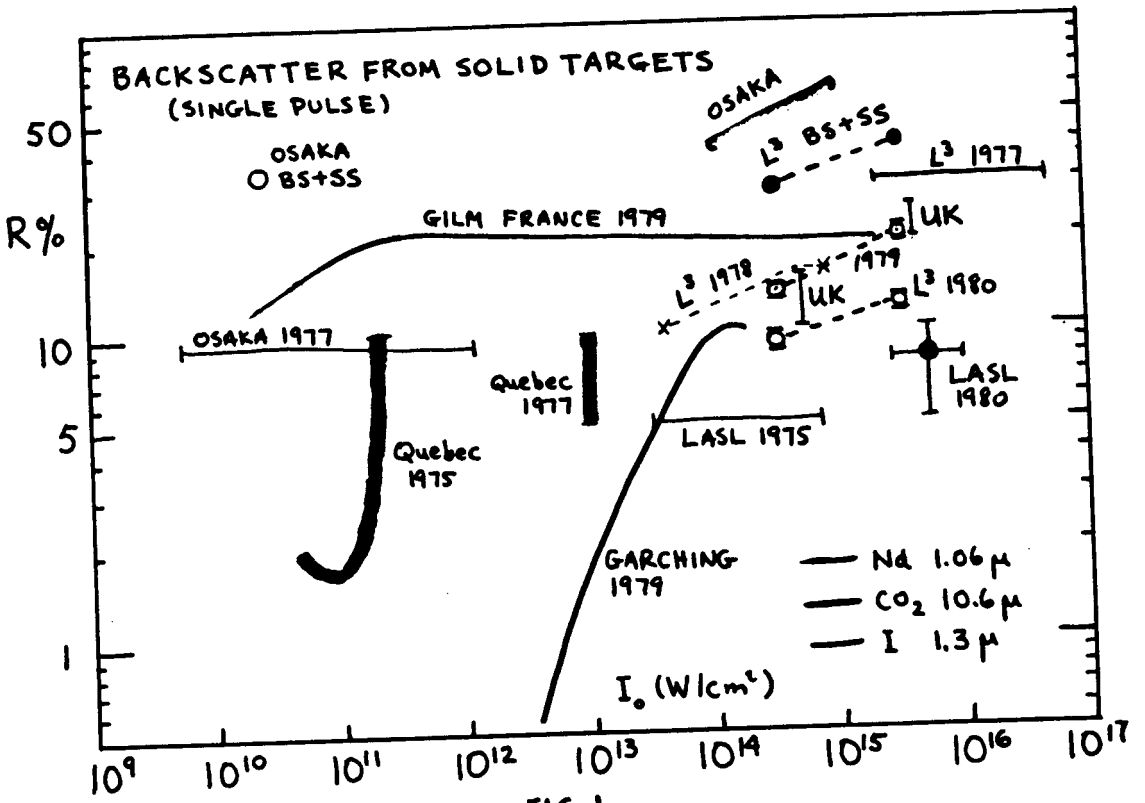
BACKSCATTER FROM SOLID TARGETS
(SINGLE PULSE)
OSAKA
BS+SS
OSAKA
L³ BS+SS
L³ 1977
R%
50
10
5
1
GILM FRANCE 1979
UK
L³ 1978
1979
UK
L³ 1980
OSAKA 1977
Quebec 1977
Quebec 1975
LASL 1980
LASL 1975
GARCHING 1979
Nd 1.06 μ
CO₂ 10.6 μ
I 1.3 μ
I₀ (W/cm²)
10⁹
10¹⁰
10¹¹
10¹²
10¹³
10¹⁴
10¹⁵
10¹⁶
10¹⁷

FIG. 1

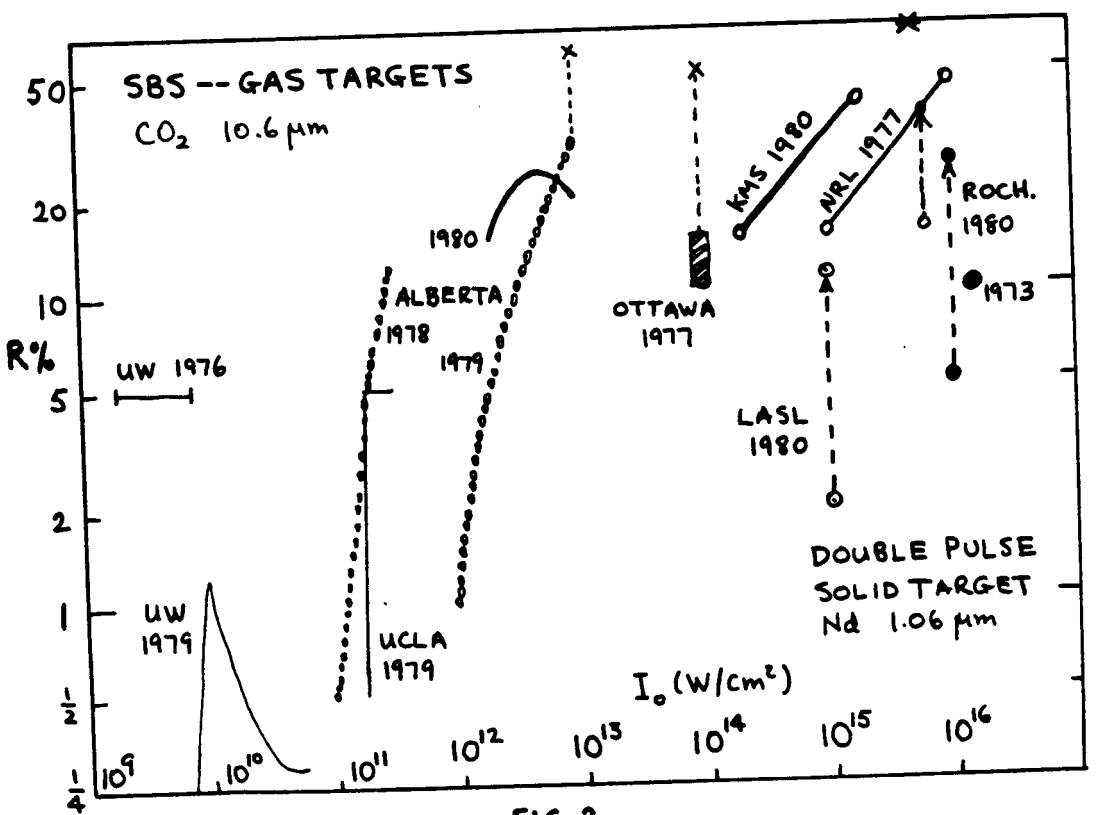
SBS -- GAS TARGETS
CO₂ 10.6 μm
50
20
10
R%
5
2
1
½
¼
1980
ALBERTA
1978
1979
UW 1976
OTTAWA
1977
KMS 1980
NRL 1977
ROCH.
1980
1973
LASL
1980
DOUBLE PULSE
SOLID TARGET
Nd 1.06 μm
UW
1979
UCLA
1979
I₀ (W/cm²)
10⁹
10¹⁰
10¹¹
10¹²
10¹³
10¹⁴
10¹⁵
10¹⁶

FIG. 2

ed to test the theory of SBS. At the Naval Research Laboratory it was shown[13] that double pulses greatly increase the backscatter (to as much as 60%) by allowing large L to develop. The scale length of n_e was measured interferometrically and taken to be L. The increase in R with prepulse amplitude is shown by the dashed lines. By varying the angle of incidence, it was determined that the scattering layer had $n \simeq 0.1 n_c$. Similar results have been obtained in double-pulse experiments at Rochester[14] (1.06 μm) and Los Alamos[15] (10.6 μm). Time-resolved spectra have been obtained at NRL[13] and ILE[14]. To the left in Fig. 2 are CO_2 data from experiments on gas or preionized plasma targets. The backscatter from arc-preionized plasmas at UCLA[16] and from magnetically confined gas breakdown plasmas at the Universities of Alberta[17] and Washington[18] are essentially in agreement, showing 5-10% maximum SBS, as in other CO_2 experiments, even at high power[7]. Unmagnetized gas breakdown plasmas at high pressures, however, have given peak reflectivities as large as 60% at Ottawa[19] and Alberta[20]. A short (double) pulse, glass laser experiment on a gas target at KMS[21] also produced large R. These experiments offer a greater degree of control of the plasma parameters than with solid targets, but they also show that SBS is extremely sensitive to the conditions created in the plasma production and heating processes.

3. Detailed Features of SBS

The experiments of Fig. 2 have verified the main features of the simple theory given above and have brought out unexpected effects. The redshift is universally found to be $\simeq 2k_o c_s$, where c_s is given by a measured T_e and a calculated T_i. The width of the spectrum is not easily interpreted if it is time-integrated, though there is a temptation to relate it to the width of the Brillouin resonance. The growth curve, R vs. I_o, usually shows a region of exponentiation followed by a saturation region. When L, n, and T_e are measured, it is possible to calculate g from Eq. (11) and show agreement[13] with Eq. (12) in the growth region. Unfortunately, T_i is never measurable and must be calculated in-

directly. By extrapolating the growth curve back to zero intensity, the initial turbulence level can be found. This is usually of order 10^{-4} times thermal noise, depending on the severity of the ionization process. Polarization of the scattered light is random near threshold but becomes linear (like the pump) as R increases[16]. In the saturation region, ion heating can account for cases where $R \geq 30\%$; but where R saturates[16,18] at $\leq 5\%$ and $10^2 < L/\lambda_o < 10^3$, more delicate mechanisms must be found, since Eq. (9) indicates saturation of the ion wave at very low amplitudes ($\simeq 1\%$).

When part of the input beam is masked off, Brillouin backscatter is found to occur only along the direction of the incident rays, even though the linear growth rate has only a weak angular dependence. Optical ray retracing has been explained[22] by the holographic pattern set up by the incident rays. Brillouin sidescatter at 90% has also been seen[16]. Because L is small in the direction transverse to the beam, the reflected light can be weak and is mixed with linear scattering from the dielectric discontinuity caused by a dense ionization front in that experiment[16], as seen by ruby-light holography. Light scattered perpendicular to the plane of $\underline{k}_o$, $\underline{E}_o$ is linearly polarized, grows as exp (I_o), and is redshifted, as is expected of SBS. Light scattered along $\underline{E}_o$ has none of these features. At low I_o, SBS is very sensitive to the plasma evolution as determined by preionization conditions. For instance, a small amount of dielectric scatter from a moving ionization front can be Brillouin amplified in a long, uniform region, giving rise to very large R at late times[16]. The seeding of SBS by a small but finite reflection has also been seen in microwave experiments[23] and can be important when a critical layer can be the reflector[24]. Finally, SBS has been found to have a spiky time structure[16,18] and frequency structure when the spectrum is time-resolved[14]; these are not yet fully explained. The dependences on ion Z and focussing f-number need also to be resolved.

4. Saturation Mechanisms

Clearly the main point of interest is the saturation level of SBS. Pump depletion and ion heating have been discussed. Wave breaking occurs only at high amplitude. Steepening of the density profile by the ponderomotive force at $n = n_c$ has been seen to limit SBS by depressing n in the underdense shelf[8,14]. Ion trapping in the wave troughs can be a large energy sink limiting wave growth. If an ion distribution $f_i(v)$ which is flat up to a velocity $(\gamma T_i/M)^{\frac{1}{2}}$ is assumed, then $\tilde{n}/n$ is limited to

$$\tilde{n}/n = \tfrac{1}{2}\{[1 + (\gamma T_i/ZT_e)]^{\frac{1}{2}} - (\gamma T_i/ZT_e)^{\frac{1}{2}}\}^2 . \qquad (17)$$

This can give small $\tilde{n}/n$, but not small enough if L/λ_o is large. However, trapping gives rise to other effects, such as a nonlinear frequency shift[25]. This can shift the wave to a region of higher linear Landau damping or, if $\tilde{n}/n$ is not uniform, the varying frequency shift can cause the coherence region L to shrink. Frequency shifts can also be caused by a strong pump. Trapping and steepening can give rise to generation of higher harmonics, which are more heavily damped. Nonlinear decay of ion waves has been suggested[26]. Two-dimensional computer simulations at Los Alamos have shown the formation of bubbles and a change in the ion wave dispersion due to electron heating by Raman scattering[27]. To find the saturation mechanisms that apply to real life is a challenge for the near future.

Acknowledgments: The author is indebted to those who provided their latest, unpublished results. This work was supported by the Los Alamos Scientific Laboratory, No. 4-XP0-1033P-1.

REFERENCES

1. W.L. Kruer and K.G. Estabrook, UCRL-83743 (1979); Laser Interaction and Related Plasma Phenomena, ed. by H.J. Schwarz and H. Hora (Plenum Press, New York, 1980), Vol. 5.
2. D. Pesme, G. Laval, and R. Pellat, Phys. Rev. Letters 31, 203 (1973).
3. J.F. Drake et al., Phys. Fluids 17, 778 (1974).
4. R.G. Evans, Rutherford Laboratory Report RL-79-061 (1979).
5. J.J. Thomson and K. Mima, Osaka Annual Report ILE-APR-78 (1978).

6. D.W. Phillion et al., Phys. Rev. Letters 39, 1529 (1977); H.D. Shay et al., Phys. Fluids 21, 1634 (1978); D.W. Phillion and M.D. Rosen, LLL Laser Program Annual Report 1978, Vol. 2, p. 5-5; M.D. Rosen et al., Phys. Fluids 22, 10 (1979).

7. K.B. Mitchell et al., Appl. Phys. Letters 27, 11 (1975); D. Casperson (private communication).

8. Osaka Institute of Laser Engineering Annual Reports 1976-77 and 1977-78.

9. D.R. Gray et al., Rutherford Laboratory preprint, 1980.

10. K. Eidmann et al., Garching report PLF-15 (1979).

11. F. Amiranoff et al., GILM preprint of paper given at APS-DPP conference, Boston, 1979.

12. H.A. Baldis et al.,Optics Commun. 15, 95 and 311 (1975); B. Grek et al., Phys.Rev. Letters 38, 898 (1977).

13. B.H. Ripin et al., Phys. Rev. Letters 39, 611 (1977) and 33, 634(1974); Appl. Phys. Letters 34, 809 (1979); and private communication.

14. R.E. Turner and L.M. Goldman, Phys. Rev. Letters 44, 400 (1980); LLE preprint (1980); L.M. Goldman et al., Phys. Rev. Letters 31, 1184 (1973).

15. D. Forslund, private communication.

16. M.J. Herbst et al., Phys. Rev. Letters 43, 1591 (1979) and UC1A PPG-382,423,424, and 446 (1979); J.J. Turechek and F.F. Chen, Phys. Rev. Letters 36, 720 (1976) and PPG-468 (1980).

17. A.A. Offenberger et al., J. Appl. Phys. 47, 1451 (1976); Optics Commun. 24, 302 (1978).

18. R. Massey et al., Phys. Rev. Letters 36, 963 (1976) and Phys. Fluids 21, 396 (1978); Z.A. Pietrzyk and T.N. Carlstrom, Appl. Phys Letters 35, 681 (1979) and private communication.

19. N.H. Burnett et al., J.Appl. Phys. 48, 3727 (1977)

20. A. Ng et al., Phys. Rev. Letters 42, 307 (1979); A.A. Offenberger, private communication.

21. F.J. Mayer et al., KMS Fusion report U-904 (1980).

22. R.H. Lehmberg, Phys. Rev. Letters 41, 863 (1978).

23. A. Mase et al., Proc. Int'l Conf. on Plasma Phys., Nagoya, 1980, Vol. I, p. 267.

24. C.J. Randall et al., Phys. Rev. Letters 43, 924 (1979).

25. H. Ikezi et al., Phys. Fluids 21, 239 (1978).

26. S. J. Karttunen and R.R.E. Salomaa, Phys. Letters 72A, 336 (1979).

27. J. Kindel, private communication.